Mendeleev Communications

Mendeleev Commun., 2025, **35**, 580–582

In situ electrolytic reduction of copper ions in the mesoporous matrices based on poly(ethylene terephthalate)

Olga V. Arzhakova,* Anastasia V. Bolshakova, Aleksandr Yu. Kopnov, Denis K. Chaplygin, Aleksandra A. Zvonova, Sofiya A. Sorochinskaya, Larisa M. Yarysheva and Alena Yu. Yarysheva

Department of Chemistry, M. V. Lomonosov Moscow State University, 119991 Moscow, Russian Federation. E-mail: arzhakova8888@gmail.com

DOI: 10.71267/mencom.7720

A simple, eco-friendly, reagent-free and cost-effective approach of *in situ* electrolytic reduction of copper sulfate that allows one to prepare copper-filled thin-film composite materials based on the mesoporous poly(ethylene terephthalate) (PET) films after their deformation *via* the mechanism of classical crazing with formation of discrete crazes with a fibrillar-porous structure is presented. The structure and properties of the copper-filled polymer materials with different levels of loading with metallic copper have been studied by X-ray analysis and scanning electron microscopy. It has been shown that metallic copper is located within the porous crazes; the degree of loading is controlled by the porosity of the PET films and it can achieve 150 wt%.

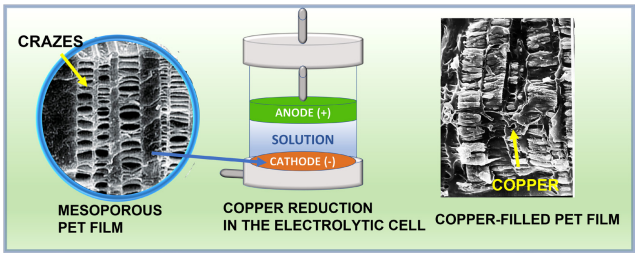

Keywords: metal-filled polymers, crazing, porosity, electrolytical reduction, composite materials, copper-filled polymers.

The development of metal-filled polymer (MFP) materials is an independent direction of modern polymer and materials science, inasmuch as the above materials are in high demand in various fields of science and technology through a combination of the properties of flexible polymer matrices and metals. A broad variety of MFPs includes electrically conductive materials, catalytic and photocatalytic systems, bioactive systems, biomedical materials (involving antibacterial and antiviral materials, systems for the targeted drug delivery, biosensors, *etc*.), photoactive systems and gas sensors, *etc*.[1–10] However, in general, the production of MFP as a combination of metals and polymers in a single system is challenged by the problems of the compatibility between thermodynamically incompatible components and phase segregation. Conventional processes of producing MFPs include two main approaches: (1) *ex situ* introduction of highly dispersed metals (nanoparticles) into melts or polymer solutions or during the polymer synthesis with subsequent molding into fibers or films and (2) *in situ* incorporation of metals *via* the reduction of metal ions from salts as precursors to a zero-valence state using redox agents or elevated temperatures within the polymers (gels and melts).[7,11,12]

This paper presents an alternative facile, cost-effective and eco-friendly approach for preparation of the MFP materials *via in situ* electrolytic reduction of copper salts to the metallic copper directly within a porous polymer matrix (PET films), thus providing the formation of a robust unified metal–polymer system. Mesoporous PET matrices (thickness of 100 microns) were prepared by the deformation of PET films in the presence of a physically active liquid environment (*n*-butanol) to various tensile strains (strain rate of 1 mm min^{-1}) *via* the mechanism of classical crazing. At low tensile strains ε (below the yield point), deformation of the PET films is accompanied by the nucleation of crazes with their unique fibrillar-porous structure according to the Rayleigh–Taylor meniscus instability mechanism (Figure 1, inset).[13–17] The resultant structure of the polymer samples is composed of alternating crazes and regions of the bulk polymer between them. As the tensile strain ε rises, craze tip advance and craze thickening come into play, and the overall porosity gradually increases (from 25% at ε = 50% to 45% at ε = 150%). Volume fraction of the porous crazes is growing, and the bulk polymer is consumed *via* a gradual transformation into the oriented fibrils in accordance with the surface drawing mechanism.[14,16] In the case of the classical crazing, the pore size (the distance between the neighboring fibrils) is independent of the tensile strain and is equal to 3 nm.

In situ electrolytic reduction of copper ions within the porous PET matrices has been performed as follows: porous PET films with fixed dimensions have been placed onto the cathode (graphite electrode) of the electrolytic cell [Figure 1(*a*)], and direct current (DC) has been applied (DC density of 900 mA cm^{-2}). The plexiglass container has been filled with a solution of copper sulfate $CuSO_4 \cdot 5H_2O$ (15 g of salt per 100 ml of water and 5 ml of ethanol). The current density on the cathode was 2–20 mA cm^{-2}. The solution was topped by the copper anode [Figure 1(*a*)]. The duration of the reduction was 1 h. After electrolysis, the samples have been carefully washed with the running distilled water and dried in vacuum under isometric conditions until a constant weight was attained.

The reduction of the copper ions into the metallic copper proceeds according to the following scheme:

$$CuSO_4 = Cu^{2+} + SO_4^{2-}$$
$$\text{Cathode: } Cu^{2+} + 2e^- \rightarrow Cu^0$$
$$\text{Anode: } Cu^0 - 2e^- \rightarrow Cu^{2+}$$

The X-ray diffraction patterns of the MFPs were collected using an URD-6 diffractometer (CuKα irradiation, wavelength

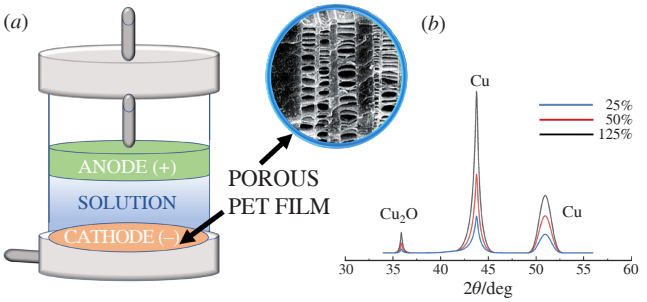

Figure 1 (*a*) Schematic representation of an electrolytic cell for the *in situ* reduction of copper ions within the porous PET film and (*b*) the diffractogram of the copper-filled MFP based on porous PET with various tensile strains. Inset: SEM micrograph of the porous PET film with discrete crazes.

λ = 1.54 Å). The peaks [Figure 1(*b*)] were identified using the reference tables of interplanar distances.[18] Two scattering maxima at angles 2θ = 43.6–43.8° and 2θ = 50.7–51° correspond to the pure copper and the first maximum at 2θ = 35.5–35.7° – to copper(I). All the diffraction peaks appeared to be in a good agreement with the standard crystal lattice of face-centered copper (JCPDS No. 040836). No peaks indicating the presence of impurities in the system have been observed. The intensity of the peaks corresponding to pure copper was much higher than those related to Cu^+. This fact clearly indicates the predominant reduction copper ions to pure copper (Cu^0) under the selected conditions. As the tensile strain rises, the intensity of the copper-assigned peaks increases, thus indicating the growth in the degree of loading. This evidence has been supported by the gravimetric measurements. According to the calculations of the Sherrer equation, the mean dimensions of crystallites are 2–4 nm. Figure 2 depicts the degree of loading plotted against the tensile strain of the porous polymer film. With the tensile strain raising, the content of the reduced copper in the PET matrix markedly increases and reaches the maximum level at ε = 150–200% (Figure 2), which is in good agreement with the porosity/tensile strain dependence.

Structure of the thin-film MFP composite materials was studied by scanning electron microscopy (SEM). Figure 3 shows the SEM micrographs of the PET samples with various tensile strains after the copper reduction (the film surface facing the anode and the cathode and the fractured surface visualizing the inner structure of copper-containing MFP).

At low tensile strains (ε = 25%), the reduced copper within the fibrillar-porous space of crazes exists as small-sized platelets which are seen on the anode- and cathode-faced surfaces and within the bulk. As the tensile strain increases to 125% (porosity is 45%), the degree of loading also increases, and copper particles are organized into a layered structure with their long axis along the fibrils. As is seen, at higher magnifications, copper exists in the platelets as individual grains or clusters and occupies the entire thickness of the film, and percolation threshold is achieved. Copper is also seen to be deposited as a thin conductive layer on the film surface. As a result, the MFP becomes electrically

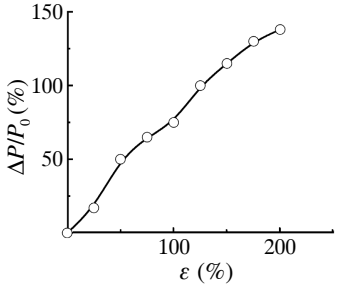

Figure 2 Copper content in the PET-based MFP *vs.* tensile strain of the PET film (butanol; classical crazing). Experimental error is 2–3%.

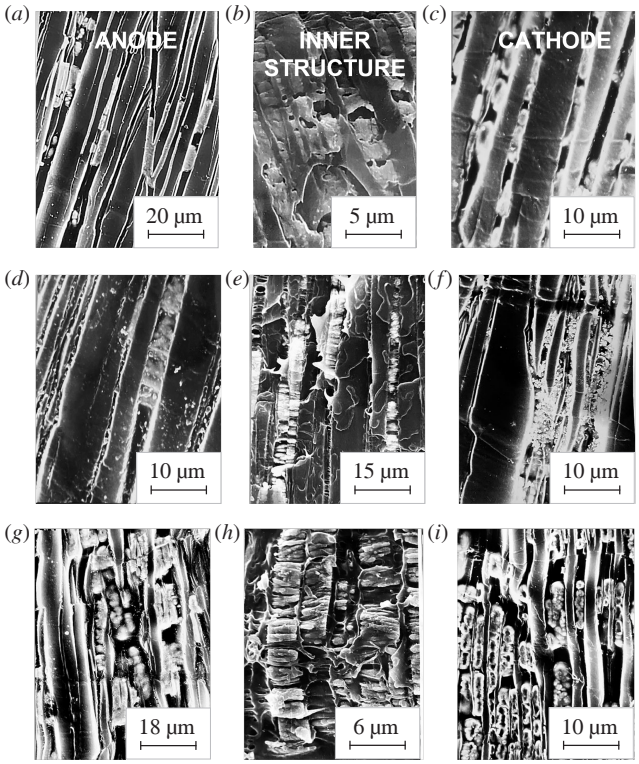

Figure 3 SEM micrographs of PET films after copper deposition: (*a*), (*d*), (*g*) from the anode side, (*b*), (*e*), (*h*) fractured surface and (*c*), (*f*), (*i*) from the cathode side. The tensile strain of the PET film: (*a*), (*b*), (*c*) ε = 25%, (*d*), (*e*), (*f*) ε = 50% and (g), (*h*), (*i*) ε = 125%.

conductive, and its specific electrical conductivity virtually approaches that of pure copper (50 MSm m^{-1}).

To summarize, this approach allows the preparation of the thin-film copper-containing MFPs based on PET with a controlled degree of loading (up to ultrahigh loading) in a facile, cost-effective, eco-friendly and reagent-free mode *via* electrolytic reduction of copper ions within the mesoporous polymer matrices. The as-prepared MFPs can be used as electro- and thermally conductive and antibacterial materials owing to the pronounced bactericidal effect of copper.

The research was carried out within the project 'Modern Problems of Chemistry and Physical Chemistry of Macromolecular Compounds' (State Assignment no. AAAA-A21-121011990022-4).

Online Supplementary Materials

Supplementary data associated with this article can be found in the online version at doi: 10.71267/mencom.7720.

References

1 Y. Yan, J. Zhang, L. Ren and C. Tang, *Chem. Soc. Rev.*, 2016, **45**, 5232; https://doi.org/10.1039/C6CS00026F.
2 L.-S. Hornberger and F. Adams, *Polymers*, 2022, **14**, 2778; https://doi.org/10.3390/polym14142778.
3 P. Strasser, U. Monkowius and I. Teasdale, *Polymer*, 2022, **246**, 124737; https://doi.org/10.1016/j.polymer.2022.124737.
4 F. Bouzat, G. Darsy, S. Foucaud and R. Lucas, *Polym. Rev.*, 2016, **56**, 187; https://doi.org/10.1080/15583724.2015.1091775.
5 M. Merkis, J. Puišo, D. Adliene and J. Laurikaitiene, *Polymers*, 2021, **13**, 3925; https://doi.org/10.3390/polym13223925.
6 F. B. Ilhami, S.-Y. Huang and C.-C. Cheng, *Acta Biomater.*, 2022, **151**, 576; https://doi.org/10.1016/j.actbio.2022.07.065.
7 A. Ghazzy, R. R. Naik and A. K. Shakya, *Polymers*, 2023, **15**, 2167; https://doi.org/10.3390/polym15092167.
8 S. Pramanik and P. Das, in *Nanomaterials and Polymer Nanocomposites*, ed. N. Karak, Elsevier, Amsterdam, 2019, pp. 91–121; https://doi.org/10.1016/B978-0-12-814615-6.00003-5.

9 L. Kong, J. Zhao, S. Han, T. Zhang, L. He, P. Zhang and S. Dai, *Ind. Eng. Chem. Res.*, 2019, **58**, 6438; https://doi.org/10.1021/acs.iecr.9b00669.
10 J. López-Molino and P. Amo-Ochoa, *ChemPlusChem*, 2020, **85**, 1564; https://doi.org/10.1002/cplu.202000428.
11 G. I. Dzhardimalieva and I. E. Uflyand, *J. Polym. Res.*, 2018, **25**, 255; https://doi.org/10.1007/s10965-018-1646-8.
12 S. Khalid and R. Nazir, in *Handbook of Polymer and Ceramic Technology*, eds. C. M. Hussain and S. Thomas, Springer, Cham, 2020, pp. 1–36; https://doi.org/10.1007/978-3-030-10614-0_78-1.
13 A. Yu. Yarysheva, L. M. Yarysheva and O. V. Arzhakova, *Mendeleev Commun.*, 2023, **33**, 259; https://doi.org/10.1016/j.mencom.2023.02.035.
14 A. Yu. Yarysheva, A. Yu. Kopnov, A. K. Berkovich, A. V. Bakirov, L. M. Yarysheva, O. V. Arzhakova and S. N. Chvalun, *Mendeleev Commun.*, 2024, **34**, 604; https://doi.org/10.1016/j.mencom.2024.06.044.
15 O. V. Arzhakova, A. Yu. Kopnov, A. I. Nazarov, A. A. Dolgova and A. L. Volynskii, *Polymer*, 2020, **186**, 122020; https://doi.org/10.1016/j.polymer.2019.122020.
16 O. V. Arzhakova, A. A. Dolgova and A. L. Volynskii, *ACS Appl. Mater. Interfaces*, 2019, **11**, 18701; https://doi.org/10.1021/acsami.9b02570.
17 A. L. Volynskii and N. F. Bakeev, *Surface Phenomena in the Structural and Mechanical Behaviour of Solid Polymers*, 1st edn., CRC Press, Boca Raton, 2016; https://doi.org/10.1201/9781315367873.
18 R. Ivanauskas, I. Ancutienė, D. Milašienė, A. Ivanauskas and A. Bronušienė, *Materials*, 2022, **15**, 7623; https://doi.org/10.3390/ma15217623.

Received: 9th January 2025; Com. 25/7720